Stem Cell Reports, Volume *11*

Supplemental Information

Excitable Adult-Generated GABAergic Neurons Acquire Functional Innervation in the Cortex after Stroke

Timal S. Kannangara, Anthony Carter, Yingben Xue, Jagroop S. Dhaliwal, Jean-Claude Béïque, and Diane C. Lagace

Supplemental Figures and Tables

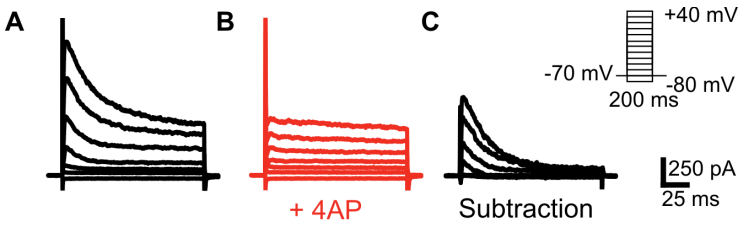

Figure S1. Nestin-GFP+ cell in the sham mouse cortex exhibit 4-AP sensitive currents. Related to Figure 1M. Example current traces recorded from a GFP+ cell in the sham surgery mouse cortex. (**A-B**) Current traces are in response to 200 ms voltage steps (-80 to +40 mV, Vh: -70 mV), prior to (**A**), and after 4AP (3mM) application (**B**). (**C**) Subtracted traces show the presence of a 4AP-sensitive early outward current (n = 3).

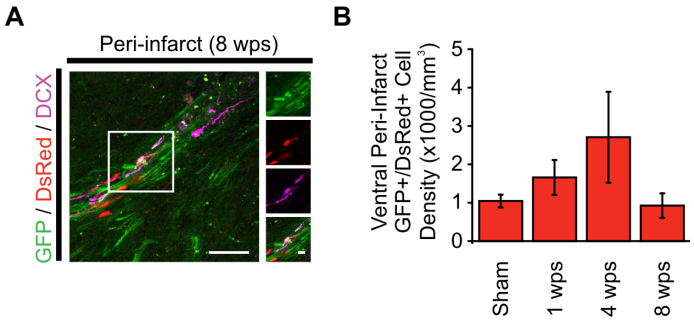

Figure S2. Decreased GFP/DsRed+ cell density in the cortex at 8 wps. Related to Figure 2. (**A**) Immunostained stroke-injured brain at 8 wps, with sparse GFP/DsRed/DCX+ cells in ventral-peri-infarct cortex (**B**) Density of cells expressing GFP/DsRed+ in the ventral peri-infarct cortex. n = 3-7 mice, Scale bars: 40 µm, 10 µm (insets). Data are represented as mean ± SEM.

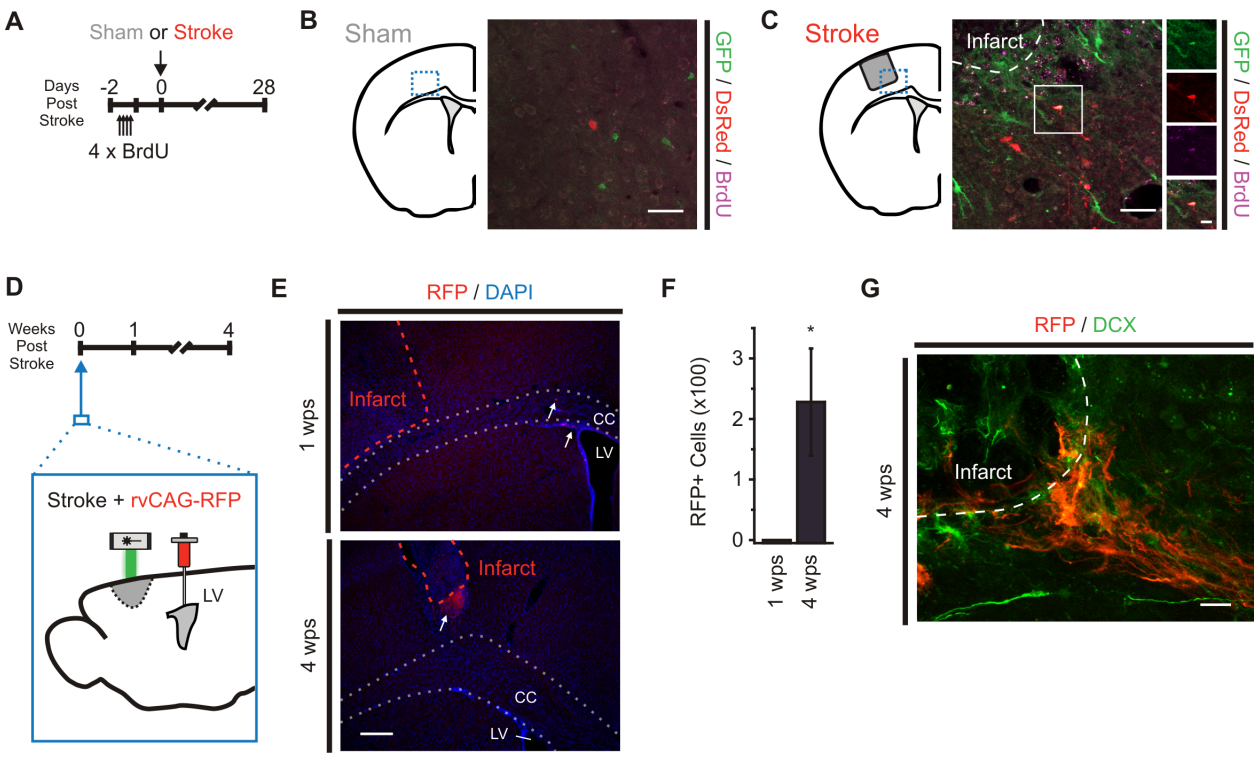

Figure S3. SVZ PCs contribute to DCX+ population at ventral peri-infarct regions. Related to Figure 2. (**A**) Schematic of experiment performed to label SVZ-PCs prior to stroke induction. (**B**) Immunostaining of sham surgery mouse cortex, four weeks after surgery. No GFP/DsRed/BrdU+ was detected (n=2). (**C**) Immunostaining of peri-infarct cortex, at 4 wps. A population of GFP/DsRed/BrdU+ could be detected (10.6 ± 5.3% of GFP/DsRed+ cells, n=4). (**D**) Schematic of experiment performed to label SVZ-PCs during stroke induction. (**E**) Immunostained stroke-injured brain, with RFP+ cells in the ventral peri-infarct cortex at 1 and 4 wps (**F**) Number of RFP+ cells identified at 1 and 4 wps in the peri-infarct cortex. (n = 2 (1 wps), 4 (4 wps), * indicates $p < 0.05$; One-Sample t-test vs. test mean) (**G**) Immunostained ventral peri-infarct cortex of a 4 wps mouse, with DCX detected in RFP+ cells. Scale bars: B, C = 40 µm, 10 µm (inset), E = 200 µm, G = 40 µm. Data are represented as mean ± SEM.

Table S1. Electrophysiological Properties of Nestin-GFP Precursor Cells in the Sham and Stroke-Injured Cortex. Related to Figure 1M-P.

GFP Cell Type	Input Resistance (IR; MΩ)	Resting Membrane Potential (RMP; mV)
Sham – Oligodendrocyte-type	58.6 ± 14.3 (n = 13)	-78.3 ± 1.8 (n = 13)
Stroke – Oligodendrocyte-type	289.1 ± 99.1 (n = 31)	-82.9 ± 1.1 (n = 30)
Stroke – Astrocyte-type	65.5 ± 7.0 (n = 7)	-82.8 ± 1.0 (n = 6)
Stroke – Neuron-type	3228.7 ± 1271.3 (n = 3)	-61.9 ± 6.2 (n = 3)

Table S2. Electrophysiological Properties of Nestin-GFP/DCX-DsRed Immature Neurons in the Stroke-Injured Cortex. Related to Figure 4.

GFP/DsRed Cell Type	Input Resistance (IR; MΩ)	Resting Membrane Potential (RMP; mV)	sPSC Amplitude (pA)	sPSC Frequency (Hz)
Class 1	6395.2 ± 803.0 (n = 21)	-56.7 ± 4.9 (n = 17)	11.6 ± 1.0 (n = 9)	0.02 ± 0.01 (n = 12)
Class 2	5346.8 ± 989.2 (n = 28)	-61.0 ± 4.7 (n = 20)	17.5 ± 2.0 (n = 14)	0.12 ± 0.05 (n = 14)
Class 3	6300.0 ± 1913.5 (n = 10)	-42.2 ± 5.8 (n = 5)	14.3 ± 1.2 (n = 7)	0.22 ± 0.06 (n = 7)

Table S3. Cells Recorded for Electrophysiological Experiments. Related to Figure 1M-P, Figure 4B, F, H, K

Figure	Experiment	# of Cells (# of Mice)
$1M_2$	IV curve	13 cells (6 mice)
$1N_2$	IV curve	31 cells (16 mice)
$1N_4$	% of GFP with oligodendrocyte-like properties	Sham: 13 cells (6 mice) 1 wps: 22 cells (8 mice) 4 wps: 9 cells (8 mice)
$1O_2$	IV curve	5 cells (4 mice)
$1O_4$	% of GFP with astrocyte-like properties	Sham: 0 cells 1 wps: 4 cells (2 mice) 4 wps: 3 cells (2 mice)
$1P_2$	% of GFP with neuron-like properties	Sham: 0 cells 1 wps: 2 cells (2 mice) 4 wps: 1 cell (1 mouse)
$4B_{1-3}$	IV curve	Class 1: 11 cells (9 mice) Class 2: 15 cells (13 mice) Class 3: 6 cells (6 mice)
4F	Evoked PSC Bicuculine	6 cells (5 mice)
$4H_1$	sPSC amplitude	Class 1: 9 cells (8 mice) Class 2: 14 cells (13 mice) Class 3: 7 cells (7 mice)
$4H_2$	sPSC frequency	Class 1: 12 cells (11 mice) Class 2: 14 cells (13 mice) Class 3: 7 cells (7 mice)
4K	sPSC Bicuculine	8 cells (6 mice)

Table S4. List of Antibodies/Primers Used. Related to Figures 1-3, S2-3.

Antibodies	Concentration Used	Source	Identifier
Chicken anti-GFP	1:5000 (mosaic images, whole-cell post hoc staining, BrdU staining, 1:50,000 for other experiments	Aves Labs	GFP-1020
Rabbit anti-DsRed	1:5000 (whole-cell post hoc staining, BrdU staining), no primary for other experiments	Clonetech	632496
Rabbit anti-OLIG2	1:500	Millipore	AB9610
Goat anti-Doublecortin	1:500	Santa Cruz	SC-8066
Mouse anti-GFAP	1:500	Millipore	MAB 3402
Mouse anti-Calretinin	1:5000	Millipore	MAB 1568
Rabbit anti-Tyrosine Hydroxylase	1:1000	Millipore	MAB 152
Rabbit anti-Calbindin	1:500	Millipore	AB1778
Rabbit anti-TBR1	1:1000	Abcam	AB31940
Rabbit anti-GAD65/67	1:500	Abcam	Ab11070
Rat anti-BrdU	1:500	AbCys	AbC117-7513
4′, 6-diamidine-2′-phenylindole dihydrochloride (DAPI)	1:10,000	Roche	10236276001
Donkey anti-Chicken CY2	1:500	Jackson Immuno.	703-546-155
Donkey anti-Rabbit CY3	1:500	Jackson Immuno.	711-585-152
Donkey anti-Goat CY3	1:500	Jackson Immuno.	705-165-147
Donkey anti-Mouse CY3	1:500	Jackson Immuno.	715-165-150
Donkey anti-Goat CY5	1:500	Jackson Immuno.	705-605-147
Donkey anti-Mouse CY5	1:500	Jackson Immuno.	715-605-150
Donkey anti-Rabbit CY5	1:500	Jackson Immuno.	711-175-152
Donkey anti-Rat CY5	1:500	Jackson Immuno.	712-175-153
Streptavidin CY5	1:200	Jackson Immuno.	016-170-084
Donkey anti-Goat Dylight 405	1:250	Jackson Immuno.	705-475-147

Gene	Genbank ID	Forward Primer (5′–3′) Reverse primer (5′–3′)	Fragment Size (bp)	Ref.
Dcx	NM_001110223	GAGTGCGCTACATTTATACCATTG TGACATTCTTGGTGTACTCAACCT	129	(Liu et al., 2009)
Gad2 (GAD65)	NM_008078.2	CATTGATAAGTGTTTGGAGCTAGCA GTGCGCAAACTAGGAGGTACAA	135	(Trifonov et al., 2014)
Gad1 (GAD67)	NM_008077	TCGATTTTTCAACCAGCTCTCTACT GTGCAATTTCATATGTGAACATATT	104	(Trifonov et al., 2014)
Slc32a1 (VGAT)	NM_009508	TCACGACAAACCCAAGATCAC GTCTTCGTTCTCCTCGTACAG	188	(Sgado et al., 2013)
Slc17a7 (VGLUT1)	NM_182993	CACAGAAAGCCCAGTTCAAC CATGTTTAGGGTGGAGGTAGC	155	(Sgado et al., 2013)
mGapdh	NM_008084	TCACCATCTTCCAGGAGCG CTGCTTCACCACCTTCTTGA	571	(Tanaka et al., 2018)

Table S5. Statistics for Figures 1-4, S4.

Figure	Type of Test	Output	P Value
1D2	Kruskal-Wallis Test	H(5) = 25.78	<0.0001
	Dunn's multiple comparison test	Lateral Sham vs. 1 wps	0.0342
		Lateral Sham vs. 4 wps	>0.9999
		Lateral 1 wps vs. 4 wps	0.8453
		Ventral Sham vs. 1 wps	0.0004
		Ventral Sham vs. 4 wps	0.0381
		Ventral 1 wps vs. 4 wps	>0.9999
1H: OLIG2	One-Way ANOVA	F(2,10) = 30.64	<0.0001
	Bonferroni Post hoc	Sham vs. 1 wps	0.0402
		Sham vs. 4 wps	<0.0001
		1 wps vs. 4 wps	0.0012
1H: GFAP	One Sample t-Test with Test Mean	1wps: t(3) = 4.0777	0.0266
		4 wps: t(3) = 4.965	0.0157
	Two Sample t-Test	1 wps vs. 4 wps: t(6) = -1.506	0.1824
1I: OLIG2	Kruskal-Wallis Test	H(2) = 9.284	0.0010
	Dunn's multiple comparison tests	Sham vs. 1 wps	0.2364
		Sham vs. 4 wps	>0.9990
		1 wps vs. 4 wps	0.0080
1I: GFAP	One Sample t-Test with Test Mean	1wps: t(3) = 3.676	0.0349
		4 wps: t(3) = 3.713	0.0340
	Two Sample t-Test	1 wps vs. 4 wps: t(6) = -1.070	0.3259
1J: OLIG2	One-Way ANOVA	F(2,10) = 33.41	<0.0001
	Bonferroni Post hoc	Sham vs. 1 wps	0.0536
		Sham vs. 4 wps	<0.0001
		1 wps vs. 4 wps	0.0006
1J: GFAP	One Sample t-Test with Test Mean	1wps: t(3) = 4.329	0.0160
		4 wps: t(3) = 6.614	0.0070
	Two Sample t-Test	1 wps vs. 4 wps: t(6) = -3.629	0.012
1J: DCX	One Sample t-Test with Test Mean	1wps: t(4) = 3.172	0.0338
		4 wps: t(6) = 2.614	0.0399
	Two Sample t-Test	1 wps vs. 4 wps: t(10) = -1.336	0.2119
1K: OLIG2	One-Way ANOVA	F(2,10) = 7.550	0.0100
	Bonferroni Post hoc	Sham vs. 1 wps	0.0420
		Sham vs. 4 wps	1.000
		1 wps vs. 4 wps	0.0160
1K: GFAP	One Sample t-Test with Test Mean	1wps: t(3) = 6.628	0.0070
		4 wps: t(3) = 4.450	0.0211
	Two Sample t-Test	1 wps vs. 4 wps: t(6) = -3.317	0.0161
1K: DCX	One Sample t-Test with Test Mean	1wps: t(4) = 2.745	0.0517
	Two Sample t-Test	4 wps: t(6) = 2.561	0.0428
		1 wps vs. 4 wps: t(10) = -1.341	0.2095
2D: DsRed-	Kruskal-Wallis test	H(2) = 0.7097	0.7237
2D: DsRed+/DCX-	Kruskal-Wallis test	H(2) = 1.186	0.5809
2D: DsRed+/ DCX+	One Sample t-Test with Test Mean	1wps: t(3) = 1.517	0.1132
		4 wps: t(6) = 1.222	0.1334
	Two Sample t-Test	1 wps vs. 4 wps: t(9) = -0.8223	0.4321
2E: GFP+/ DsRed+	Kruskal-Wallis test	H(2) = 0.2045	0.9187

2E: GFP+/DsRed+/ DCX+	One Sample t-Test with Test Mean Two Sample t-Test	1wps: t(3) = 1.617 4 wps: t(6) = 1.409 1 wps vs. 4 wps: t(9) = 0.8994	0.1021 0.1043 0.3919
2F: DsRed-	Kruskal-Wallis test	H(2) = 5.318	0.0597
2F: DsRed+/ DCX-	One-Way ANOVA	F(2,11) = 3.532	0.0654
2F: DsRed+/DCX+	One Sample t-Test with Test Mean Two Sample t-Test	1wps: t(3) = 2.823 4 wps: t(6) = 2.865 1 wps vs. 4 wps: t(9) = -1.897	0.0333 0.0143 0.0903
2G: GFP+/DsRed+	Kruskal-Wallis test	H(2) = 0.5327	0.7823
2G: GFP+/DsRed+/ DCX+	One Sample t-Test with Test Mean Two Sample t-Test	1wps: t(3) = 2.529 4 wps: t(6) = 2.003 1 wps vs. 4 wps: t(9) = -1.018	0.0427 0.0461 0.3355
4H1: Amp. of sPSCs	Kruskal-Wallis test	H(2) = 3.768	0.1520
4H2: Freq. of sPSCs	Kruskal-Wallis Test Dunn's multiple comparison tests	H(2) = 12.77 Class 1 vs. 2 Class 1 vs. 3 Class 2 vs. 3	0.0017 0.1812 0.0011 0.1186
4F	Paired Sample t-Test	t(5) = 4.700	0.0053
4K	Paired Sample t-Test	t(7) = 2.865	0.0242
S4F	One Sample t-Test with Test Mean	t(3) = 3.586	0.0186

Supplemental Experimental Procedures

Animals. Mice (5-9 weeks old) were group housed in standard laboratory cages and maintained on a 12-hour light/dark cycle with access to food and water ad libitum. Nestin-GFP (B6.Cg-Tg(Nes-EGFP)1Yamm) (Yamaguchi et al., 2000), DCX-DsRed (Couillard-Despres et al., 2006) were genotyped based on previously published protocols. Breeding homozygous Nestin-GFP and DCX-DsRed mice generated the bi-transgenic reporter mice line (Nestin-GFP/DCX-DsRed). Animal procedures were approved by the University of Ottawa Animal Care Committee and adhered to the guidelines set forth by the Canadian Council on Animal Care.

Photothrombosis. Focal ischemic infarcts were produced using a modified version of the photothrombotic stroke model (Watson et al., 1985). Briefly, mice were anesthetized with 1.5-2% isofluorane and fitted to a stereotaxic apparatus. Body temperature was maintained at 37.0 ± 1.0^{o}C. Mice received a single intraperitoneal injection of 1% Rose Bengal dye (sc-203757; 100 mg/kg, in 1x PBS). After 5 minutes, the exposed skull above the sensorimotor cortex (+1 mm anterior/posterior, +2.7 mm medial/lateral to bregma) was illuminated with a green laser beam generated by a diode pumped solid-state laser (~20mW, 532 nm, Beta Electronics) for 10 minutes. Sham animals received Rose Bengal administration without laser exposure.

Retrovirus Injection. Retrovirus generation and stereotaxic injection was performed as previously described (Ceizar et al., 2016; Tashiro et al., 2006). The CAG-RFP retroviral vector, and corresponding packing and envelope construct, was generously provided by Dr. Fred Gage (The Salk Institute, La Jolla, CA, USA). RFP virus titer was determined by live tittering using 293T cells and was measured to be 1.2×10^{9} infectious units (IU) per ml. RFP virus (1.5 µl) was stereotaxically injected (0.2 µl/minute) into the apex of the SVZ (-0.7 mm anterior/posterior, +1.2 mm medial/lateral, -1.9 mm dorsal/ventral to bregma) using a 33G needle (model: 7803-05) and 10 µl gastight microsyringe (model: 1700), attached to a Hamilton (Hamilton Company). Injection was performed approximately 10 minutes following photothrombotic stroke induction.

Bromodeoxyuridine (BrdU) Injection. Pulse BrdU injections were performed as previously described (Dhaliwal et al., 2015). Mice received four intraperitoneal injections of 50 mg/kg BrdU (10 mg/mL dissolve in saline; Fluka Analytical, Sigma- Aldrich Chemie), with each injection spaced by three hours. Two days later, mice received either a sham or stroke surgery.

Tissue Collection. Mice were anesthetized with Euthanyl and transcardially perfused with cold 1x PBS and 4% paraformaldehyde (in 1x PBS) at ~ 7 mL/minute. Brains were removed, post-fixed in 4% paraformaldehyde for 1 hour, and then placed in 30% sucrose (in 1x PBS) at 4^{o}C. Coronal tissue sections (40 µm) were generated with a Leica SM 2000 R sliding microtome (Leica Microsystems), and stored as a 1:9 series, in 1x PBS (with 0.01% sodium azide) at 4^{o}C.

Immunohistochemical Detection. Free-floating sections were processed for fluorescent immunohistochemistry as previously published (Ceizar et al., 2016; Dhaliwal et al., 2015), using primary and secondary antibodies listed in the **Table S4**. Briefly, sections were washed in 1x PBS (3 x 5 minutes), and incubated in 0.1% Tween-20 and 0.1% TritonX-100 in 1x PBS with corresponding primary antibodies, on a shaker at 4^{o}C, overnight. The following day, sections were washed in 1x PBS (3 x 5 minutes), and incubated in 0.1% Tween-20 and 0.1% TritonX-100 in 1x PBS with corresponding secondary antibodies, on a shaker at room temperature, for one to two hours. Sections were counterstained with the nuclear counterstain DAPI (4′, 6-diamidine-2′-phenylindole dihydrochloride) for 2.5 minutes to aid visualization. Alterations to the set protocol were made for 1) BrdU immunodetection experiments, where an acid pre-treatment step (1N HCl in 1x PBS, at 45^{o}C for 30 minutes(Kee et al., 2007)), and 1xPBS wash (3 x 5 minutes) were performed prior to primary antibody incubation, and DAPI counterstaining was extended to a five minute incubation, and 2) the quadruple-labeling experiment, where the goat anti-doublecortin antibody was visualized using a secondary conjugated to Dylight 405, and DAPI counterstaining was excluded. Sections were mounted onto Superfrost microscope slides and coverslipped with Immunomount (Fisher Scientific).

Imaging and Histological Quantification of Fluorescent Cells. Cells were quantified in the peri-infarct region, defined as a 250 µm wide zone surrounding the necrotic border of the infarct. Counting and co-localization was performed by semi-randomly placing four sampling boxes (210 x 210 µm) in the four regions surrounding the infarct. Cells in the corpus callosum were excluded from analysis. For each sampling box, confocal image stacks

using a Zeiss LSM510/AxioImager.M1 confocal microscope with a 40x oil immersion objective (N.A. = 1.3) were collected (optical slice: 1 μm at minimum; sequential excitation at 488, 543 and 633 nm). To image quadruple-labeled cells, a Zeiss LSM510 META/AxioVert 200 confocal microscope with a 40x oil objective (N.A. = 1.3) was used (optical slice: 1 μm at minimum; sequential excitation at 405, 488, 543 and 633 nm). For tile-scanned image in Figure 1A-C, tiles were acquired using a Zeiss LSM800/AxioObserver Z1 confocal microscope with a 10x objective (N.A. = 0.3).

Fluorescence-Activated Cell Sorting (FACS) Analysis and PCR. Nestin-GFP/DCX-DsRed mice were deeply anesthetized with isofluorane (Baxter Corporation, Canada). Mice were then decapitated, and their brains were placed in oxygenated artificial cerebrebrospinal fluid used for FACS (FACS-aCSF), consisting of (in mM): 124 NaCl, 5 KCl, 1.3 MgCl2 · 6H2O, 2 CaCl2 · 2H2O, 26 NaHCO3, and 1X penicillin-streptomycin (10,000 U/mL; ThermoFisher) (pH = 7.4). Coronal sections (1.0 mm) were generated using an Adult Mouse Brain Slicer Matrix (Zivic Instruments) and sterile razor blades. Cortical regions neighbouring the stroke-induced infract were isolated using a sterile scalpel and a Zeiss SteREO Discovery.V8 dissecting scope, transferred to eppendorf tubes with minimal amount of FACS-aCSF, and gently chopped using a sterile scalpel blade. Tissue was spun down and incubated (ten minutes, 37^{o}C) in 500 uL/tube of digestion media, containing: 20 U/mL papain (Worthington Biochemicals), 12 mM EGTA (Invitrogen) in DMEM:F12 (Invitrogen). Following incubation, Resuspension Media (0.05 mg/mL DNase1 (Roche), 10% fetal bovine serum (Wisent Bioproducts) in DMEM:F12 phenol-free medium) was added to each tube and incubated for five minutes. Supernatant was then transferred in Percoll media, consisting of 19.8% Percoll (GE Healthcare Life Sciences), 2.2% 10xPBS (Wisent Bioproducts) in Resuspension Media. Cells were then spun down (500 x g, 12.5 minutes, 4^{o}C), dissolved in DMEM:F12 phenol-free medium, and sorted using a MoFlo Astrios EQ (Beckman Coulter Canada) for GFP(488-526 nm) and DsRed (561-579 nm). mRNA was extracted using Arcturus Picopure RNA Isolation Kit (Applied Biosystems; ThermoFisher) and examined for quality and quantity using an AATI Fragment Analyzer (Advanced Analytical Technologies, Inc.). Primers used for amplification are listed in **Table S4**, and were purchased from Integrated DNA Technologies, Inc. RT-PCR was completed using 300 pg mRNA and the OneStep RT-PCR kit (Qiagen, Inc.).

Whole-Cell Electrophysiology. Whole-cell electrophysiology was performed as previously described (Geddes et al., 2016; Kannangara et al., 2015; Lee et al., 2016). Mice were deeply anesthetized with isofluorane (Baxter Corporation, Canada), and transcardially perfused with ice-cold, oxygenated choline-based artificial cerebrebrospinal fluid (choline-aCSF), containing the following: 119 choline-Cl, 2.5 KCl, 4.3 MgSO4, 1.0 NaH2PO4, 1.0 CaCl2, 11 glucose, and 26.2 NaHCO3 (pH 7.2-4). Mice were then decapitated and the brain was quickly removed. Coronal slices (300 μm), containing the full extent of the infarct, were generated using a Leica VT1000 S vibratome blade microtome (Leica Microsystems). Since photothrombotic infarcts transition to become a substantial plug of necrotic tissue by four weeks post stroke, agar blocks (3%) were mounted behind the brain tissue to maintain slice integrity during the slicing procedure. Brain sections were then transferred to an incubation chamber, and allowed to recover for at least 1 hour in oxygenated artificial cerebrospinal fluid (aCSF), containing the following: 119 NaCl, 2.5 KCl, 1.3 MgSO4, 1.0 NaH2PO4, 2.5 CaCl2, 11 glucose, and 26.2 NaHCO3 (pH = 7.2-4) initially maintained at 30^{o}C, then recovered at room temperature. Slices were transferred to a perfusion chamber and perfused with oxygenated aCSF (2 mL/minute) at room temperature. Borosilicate recording pipettes (4-8 MΩ, World Precision Instruments), pulled with a PC-10 pipette puller (Narishige, Japan) were backfilled with a potassium-based intracellular solution contained the following (in mM): 115 K-gluconate, 20 KCl, 10 HEPES, 4 Mg-ATP, 0.5 tris-GTP (Na salt hydrate) and 10 Na-phosphocreatine (pH 7.23-25, adjusted with KOH; 280–290 mOsm/L). In some experiments, the internal solution was supplemented with either the fluorophore Alexa 594 hydrazide (A10438; 0.03 mM, Na-salt, Molecular Probes) or Neurobiotin (SP-1120-50; 3 mM, Vector Laboratories). Cells were targeted using a Zeiss Axio Examiner D1 upright microscope using either a 20x (1.0 NA) or 40x (1.0 NA) objective. For voltage clamp recordings, we monitored access resistance by applying a 100 ms, 5 mV hyperpolarizing pulse prior to each sweep. Recordings were discarded if access resistance changed by > 30%. Liquid junction potentials were not compensated for. To measure post-synaptic currents (PSCs), single square pulses (100 μs) were evoked with an aCSF-filled borosilicate pipette (3-4 MΩ, World Precision Instruments), driven by an ISO-flex stimulation isolation unit (A.M.P.I), at 0.1 Hz. Spontaneous post-synaptic currents (sPSCs) were recording at -70 mV in normal aCSF. In some experiments, we bath applied -(-) bicuculline methiodide (Bic, ab120108; 20 μm, Abcam) to block $GABA_AR$-mediated currents. For a subset of experiments, two-photon imaging was performed to visualize the morphology of cell types. Imaging was conducted using a Ti:Sapphire pulsed laser tuned to 850 nm (MaiTai-DeepSee, Spectra Physics) coupled to a Zeiss LSM710 multiphoton microscope with a 20x (1.0 NA) objective.

Data and Statistical Analysis. All electrophysiological recordings were analyzed using Clampfit (Molecular Devices) and OriginPro 8.5 (OriginLab). sPSCs were analyzed using a sPSC current-template search through Clampfit. Results were processed using Microsoft Excel and statistical analysis was conducted using OriginPro 8.5 and GraphPad Prism 6 (Graphpad Software). For all studies, data was presented as mean ± standard error of the mean (SEM). Single variable data was analyzed using either a one-sample t-test (when comparing to a group that had a variance = 0) or a two-tailed two-sample student's t-test, while analysis for more than one variable was analyzed using an Analysis of variance (ANOVA) followed by a Bonferroni post hoc test. Data sets failing ANOVA assumptions were analyzed using Kruskal-Wallis tests with Geisser Greenhouse corrections, and Dunn's multiple comparison tests. Differences were considered to be statistically significant when $p < 0.05$. Statistical tests are reported in **Table S5**.

Supplemental References

Ceizar, M., Dhaliwal, J., Xi, Y., Smallwood, M., Kumar, K.L., and Lagace, D.C. (2016). Bcl-2 is required for the survival of doublecortin-expressing immature neurons. Hippocampus *26*, 211-219.

Couillard-Despres, S., Winner, B., Karl, C., Lindemann, G., Schmid, P., Aigner, R., Laemke, J., Bogdahn, U., Winkler, J., Bischofberger, J.*, et al.* (2006). Targeted transgene expression in neuronal precursors: watching young neurons in the old brain. Eur J Neurosci *24*, 1535-1545.

Dhaliwal, J., Xi, Y., Bruel-Jungerman, E., Germain, J., Francis, F., and Lagace, D.C. (2015). Doublecortin (DCX) is not Essential for Survival and Differentiation of Newborn Neurons in the Adult Mouse Dentate Gyrus. Front Neurosci *9*, 494.

Geddes, S.D., Assadzada, S., Lemelin, D., Sokolovski, A., Bergeron, R., Haj-Dahmane, S., and Beique, J.C. (2016). Target-specific modulation of the descending prefrontal cortex inputs to the dorsal raphe nucleus by cannabinoids. Proc Natl Acad Sci U S A *113*, 5429-5434.

Kannangara, T.S., Eadie, B.D., Bostrom, C.A., Morch, K., Brocardo, P.S., and Christie, B.R. (2015). GluN2A-/- Mice Lack Bidirectional Synaptic Plasticity in the Dentate Gyrus and Perform Poorly on Spatial Pattern Separation Tasks. Cereb Cortex *25*, 2102-2113.

Kee, N., Teixeira, C.M., Wang, A.H., and Frankland, P.W. (2007). Preferential incorporation of adult-generated granule cells into spatial memory networks in the dentate gyrus. Nat Neurosci *10*, 355-362.

Lee, K.F., Soares, C., Thivierge, J.P., and Beique, J.C. (2016). Correlated Synaptic Inputs Drive Dendritic Calcium Amplification and Cooperative Plasticity during Clustered Synapse Development. Neuron *89*, 784-799.

Liu, X.S., Chopp, M., Zhang, X.G., Zhang, R.L., Buller, B., Hozeska-Solgot, A., Gregg, S.R., and Zhang, Z.G. (2009). Gene profiles and electrophysiology of doublecortin-expressing cells in the subventricular zone after ischemic stroke. J Cereb Blood Flow Metab *29*, 297-307.

Sgado, P., Genovesi, S., Kalinovsky, A., Zunino, G., Macchi, F., Allegra, M., Murenu, E., Provenzano, G., Tripathi, P.P., Casarosa, S.*, et al.* (2013). Loss of GABAergic neurons in the hippocampus and cerebral cortex of Engrailed-2 null mutant mice: implications for autism spectrum disorders. Exp Neurol *247*, 496-505.

Tanaka, K.I., Xue, Y., Nguyen-Yamamoto, L., Morris, J.A., Kanazawa, I., Sugimoto, T., Wing, S.S., Richards, J.B., and Goltzman, D. (2018). FAM210A is a novel determinant of bone and muscle structure and strength. Proc Natl Acad Sci U S A.

Tashiro, A., Sandler, V.M., Toni, N., Zhao, C., and Gage, F.H. (2006). NMDA-receptor-mediated, cell-specific integration of new neurons in adult dentate gyrus. Nature *442*, 929-933.

Trifonov, S., Yamashita, Y., Kase, M., Maruyama, M., and Sugimoto, T. (2014). Glutamic acid decarboxylase 1 alternative splicing isoforms: characterization, expression and quantification in the mouse brain. BMC Neurosci *15*, 114.

Watson, B.D., Dietrich, W.D., Busto, R., Wachtel, M.S., and Ginsberg, M.D. (1985). Induction of reproducible brain infarction by photochemically initiated thrombosis. Ann Neurol *17*, 497-504.

Yamaguchi, M., Saito, H., Suzuki, M., and Mori, K. (2000). Visualization of neurogenesis in the central nervous system using nestin promoter-GFP transgenic mice. Neuroreport *11*, 1991-1996.